



Effects of *Pinus taeda* leaf anatomy on vascular and extravascular leaf hydraulic conductance as influenced by N-fertilization and elevated CO₂

Jean-Christophe Domec^{1,2}, Sari Palmroth², and Ram Oren²

¹Bordeaux Sciences Agro, UMR 1391 INRA-ISPA, 33175 Gradignan Cedex, France; ²Nicholas School of the Environment, Box 90328, Duke University, Durham, NC 27708, USA

Corresponding author: Jean-Christophe Domec, jc.domec@agro-bordeaux.fr

Date of submission: December 18, 2015

Date of publication: March 26, 2015

Abstract

Silvicultural practices (e.g., nitrogen addition through fertilization) and environmental changes (e.g., elevated [CO₂]) may alter needle structure, impacting mass and energy exchange between the biosphere and atmosphere through alteration of stomatal function. Hydraulic resistances in leaves, controlling the mass and energy exchanges, occur both in the xylem and in the flow paths across the mesophyll to evaporation sites, and therefore largely depends on the structure of the leaf. We used the Free-Air Carbon dioxide Enrichment (FACE) experiment, providing a unique setting for assessing the interaction effects of [CO₂] and nitrogen (N) supply to examine how leaf morphological and anatomical characteristics control leaf hydraulic conductance (K_{leaf}) of loblolly pine (*Pinus taeda* L.) trees subjected to ambient or elevated (+200 ppmv) CO₂ concentrations (CO₂^a and CO₂^e, respectively) and to soil nitrogen amendment (N). Our study revealed that CO₂^e decreased the number of tracheids per needle, and increased the distance from the xylem vascular bundle to the stomata cavities, perturbing the leaf hydraulic system. Both treatments induced a decrease in K_{leaf} , and CO₂^e also decreased leaf extravascular conductance ($K_{\text{extravascular}}$), the conductance to water flow from the xylem to the leaf-internal air space. Decline in K_{leaf} under CO₂^e was driven by the decline in $K_{\text{extravascular}}$, potentially due to longer path for water movement through the mesophyll, explaining the decline in stomatal conductance (g_s) observed under CO₂^e. This suggests that the distance from vascular conduits to stomata sub-cavity was a major constraint of leaf water transport. Across treatments our results showed that needle vein conductivity was slightly more limited by the lumen than by the bordered-pits, the latter accounting for 30-45% of vein resistance. CO₂^e-induced reduction in K_{leaf} was also consistent with an increased resistance to xylem collapse due to thicker cell wall. In addition, stomatal closure corresponded to the water potential inducing a reduction in 50% of leaf vascular conductance (K_{vascular}) via xylem wall rupture. The water potential that was estimated to induce complete xylem wall collapse was related to the water potential at turgor loss. Our study provided a framework for understanding the interaction between CO₂^e and N availability in affecting leaf anatomy, and the mechanisms for the response of K_{leaf} to the treatments. These mechanisms can be incorporated into predictive models of g_s , critical for estimating forest productivity in water limited environments in current and future climates and a landscape composed of sites of a range in soil N fertility.

Keywords: extravascular leaf conductance, FACE, leaf anatomy, *Pinus taeda* L., turgor loss

Introduction

Water flow in the soil-plant-atmosphere continuum is determined by the whole-plant hydraulic conductance from soil through plant tissues (K_{plant}), characterizing the structural capacity of the plant for water flow (Zimmermann 1983). Changes in K_{plant} related to changes in size (McCulloh et al. 2015), drought (Meinzer et al. 2003, Brodribb and Holbrook 2003, Addington et al. 2004, Domec and Pruyn 2008), fertilization (Bucci et al. 2006), elevated CO_2 (CO_2°) concentration (Domec et al. 2010) have been linked to variation in gas exchange, carbon uptake and growth. For the last fifteen years, plant physiologists have come to appreciate the influence that leaves make to K_{plant} , and their importance to understanding scaling physiological processes within plants (Brodribb and Holbrook 2004, Sacks and Holbrook 2006, Johnson et al. 2011, McCulloh et al. 2015).

Past studies showed that, in *Pinus taeda*, leaf hydraulic conductance (K_{leaf}) was strongly correlated with K_{plant} among trees exposed to a range in resource availabilities imposed by soil nitrogen amendment (N) and CO_2° (Domec et al. 2009a, Tor-ngern et al. 2015). Because leaves represented a substantial component of K_{plant} , reduction in K_{leaf} under CO_2° appeared to impose a decline in the efficiency of water conduction through the plant, thus affecting leaf gas exchange and tree transpiration over the long term. In *P. taeda*, a recent short-term manipulations in CO_2° caused no direct response in stomatal functioning, and the observation of long-term 21% reduction in stomatal conductance (g_s) was consistent with the indirect effect of decreased K_{leaf} and increased mutual shading, the latter associated with greater leaf area index (Tor-ngern et al. 2015). The differences in the CO_2° x fertilized response of K_{leaf} may potentially be related to the characteristic differences in the development of conducting tissue effects of the treatments on plant ontogeny (Pritchard et al. 1999, Lin et al. 2001). Although leaf morphological features have been assessed for their contribution to plant responses to N-fertilization and CO_2° (Thomas and Harvery 1991, Lin et al. 2001, Maier et al. 2008), information on such responses is still limited. The responses of leaf anatomy to rising CO_2° and to fertilization has already been quantified, but most studies have focused on stomatal structure and density (Radoglou and Jarvis 1990, Woodward and Kelly 1995, Reid et al. 2007), and no data are available on anatomical characteristics of the leaf xylem of trees growing under future CO_2 conditions, especially in relation to K_{leaf} .

Xylem structure determines the hydraulic efficiency and safety of a particular plant organ (Zimmermann 1983, Hacke et al. 2005), providing the structural basis for gas exchange regulation. In leaves, water exits the xylem veins through the bundle sheath cells and then across the endodermis to the mesophyll where it evaporates and then diffuses through the stomata (Leegood 2008). In conifers, the needle vein architecture is very simple, consisting of a single unbranched strand of xylem and phloem surrounded by transfusion tissue. The vascular tissues are separated from the chlorophyll-containing mesophyll by an endodermis consisting of casparian strips. Leaf hydraulic conductance measures the contribution of both vascular and extravascular pathways for water movement inside leaves. Several studies have revealed that the hydraulic resistances of the vascular and extravascular compartments are of the same order of magnitude and vary depending on species and environmental conditions (Zwieniecki et al. 2002, Sack and Tyree 2005, Nardini and Salleo 2005). Reduction in K_{leaf} following a decline in leaf water status, have been shown to reflect a reduction in the leaf vascular hydraulic conductance (K_{vascular}) via xylem cavitation in veins (Bucci et al. 2003, Nardini et al. 2003, Johnson et al. 2009, 2012). However, other studies showed that the reduction in K_{leaf} was more of a consequence of the reduction in extravascular leaf hydraulic conductance ($K_{\text{extravascular}}$) (Charra-Vaskou et al. 2012, Scoffoni 2015, Bouche et al. 2015). Variations in transfusion tissue, mesophyll area, and distance from vascular conduits to stomata sub-cavity is viewed as a possible determinant of $K_{\text{extravascular}}$ (Aasamaa et al. 2001, Sack et al. 2003, Brodribb et al. 2007). Yet, it is still unclear which leaf structural features drive the functional differences in $K_{\text{extravascular}}$ and K_{vascular} among treatments (Buckley 2015, Sack et al. 2015). These data may be necessary to discriminate between the responses of leaf mesophyll and vascular tissues to CO_2° , and thus for bridging data collected at fine, physiological level to whole-plant processes. In angiosperms, K_{vascular} can be determined by cutting subsequent vein orders until the increase of K_{leaf} converges on the expected vascular conductance (Nardini and Salleo 2005, Coomes et al. 2008). For conifers, the lack of distinct veins requires an alternative method which disrupts the living structures of the leaf by freezing or boiling the entire organ. The measured conductance is then reduced to its vascular component (Tyree and Nardini 2001, Cochard et al. 2004a).

Tracheid anatomical data can also be useful in determining hydraulic failure by xylem wall collapse (implosion) under tension, because it is simply a function of tracheid cell wall thickness in relation to the lumen diameter (Hacke et al. 2001, Pittermann et al. 2006, Rosner et al. 2016). In lignified plant organs, simple calculations have suggested that the pressure differentials between adjacent water- and air-filled conduits are not sufficient to cause rupture of lignified cell walls (Rundel and Stecker 1977, Jacobsen et al. 2005, Domec et al. 2009b). Because leaves possess numerous air space and experience large pressure differentials across cell walls, a decrease of K_{vascular} in dehydrating pine needles due to tracheid collapse has been shown to be plausible (Cochard et al. 2004b), although a recent study showed otherwise with deformation of tracheid walls occurring only in seedlings, but not in matures trees (Bouche et al. 2015). Wall collapse reduces lumen area and considerably increases tracheid hydraulic resistance

to water flow, thus impacting K_{vascular} (Brodribb and Holbrook 2005). Based on these considerations, if leaf anatomical traits adjust to variation in resource availabilities (CO_2^e and/or N-fertilization), this should be reflected in changes in leaf hydraulic capabilities and consequently in g_s .

Long-term treatments of CO_2^e and N-fertilization perturbed the hydraulic system, allowing a test of how broadly influences of leaf structural characteristics hold outside the range found under typical conditions. We investigated the structural and anatomical basis for the decreased in K_{leaf} and its higher sensitivity to leaf water potential in the $\text{CO}_2^e \times \text{N}$ -fertilized trees. Specifically, we hypothesize that: 1) acclimations in xylem vascular structure and, thus, in K_{vascular} dominates the difference in K_{leaf} under CO_2^e and/or N-fertilization; 2) lower K_{leaf} in trees growing under CO_2^e and N is associated with an increased in xylem wall resistance to collapse, and the water potential at turgor loss; and 3) variations in mesophyll area and distance from vascular conduits to stomata sub-cavity is correlated with $K_{\text{extravascular}}$, which also constraints K_{leaf} and g_s . To test these hypotheses we measured needle anatomical and hydraulic properties of trees growing under fertilization and CO_2^e (Duke free-air CO_2 enrichment: FACE) and compared these traits to published values of water potential at turgor loss and g_s measured on the same trees (Domec et al. 2009a).

Materials and Methods

Experimental setting

The experiment was located in a loblolly pine (*Pinus taeda* L.) plantation established in 1983 on low fertility, acidic clay-loam of the Enon series, in the Blackwood Division of Duke Forest, North Carolina ($35^{\circ}58' \text{N}$, $79^{\circ}08' \text{W}$). The experimental site consisted of four plots exposed to ambient CO_2 (CO_2^a) and four plots targeted at $+200 \text{ mmol mol}^{-1}$ CO_2 (CO_2^e) above current, with half of each plot fertilized with nitrogen (Oren et al. 2001, Schäfer et al. 2002). CO_2 enrichment was implemented according to the free-air CO_2 enrichment (FACE) protocol throughout the year whenever ambient temperature was above 5°C and wind speed was below 5 m s^{-1} . In 1994, two 30-m diameter plots were established: the FACE prototype plot (Plot 7) and its adjacent untreated reference plot (Plot 8) were established, three of which received CO_2^e . The other three enriched plots, and their references began operating in 1996. In 1998, the prototype plot and its reference plot were halved using a ditch and a barrier, and one-half of each has received annual nitrogen fertilization (N) of 11.2 g N m^{-2} (Oren et al. 2001); the same design was implemented in the rest of the plots in 2005.

Leaf structure and anatomy

Due to the difficulty in sampling upper crown needles from each tower in each of the rings, two upper canopy shoots from one tree per ring were sampled for a total of eight current-year needles for each treatment combination. Physical needles characteristics measured included needle length, width, thickness and area, as well as needle density and mass per area (Table 1, Supplementary Figure 1). Samples were then oven-dried at 65°C for 48 h. Fresh needle areas and volume were obtained geometrically (assuming a needle is a third of a cylinder) from dimensions of length and width measured using a digital caliper (series 500 Mitutoyo, Aurora, IL, USA) and a graduated hand lens (Rundel and Yoder 1998). Needle mass per area (g m^{-2}) was determined as the ratio of dry mass to total green needle area. Needle density (g m^{-3}) was calculated as the ratio of dried weight over fresh volume.

Anatomical features were determined from transverse sections made with a sliding microtome and taken in the middle region of the samples. The sections were then stained with aqueous toluidine blue and mounted on a glass slide with glycerin. We photographed the sections at 40x and 400x magnification with a digital camera mounted on a microscope and analyzed the images using the software Image-J 136b (National Institutes of Health, MD, USA). Images taken at 40x were used to determine the circumference of the needles, the area of the mesophyll and the area surrounded by the endodermis cells that comprises the transfusion tissue and the vascular bundle (phloem and xylem). Images taken at 400x were used to determine the number and the size (lumen, cell wall) of each tracheid within the xylem area. To test whether mesophyll area and distance from vascular conduits to stomata sub-cavity was viewed as a possible constraint on K_{leaf} , the xylem pathway through the leaf mesophyll was quantified by measuring the linear path length from the xylem to stomata as described in Brodribb et al. (2007). Mean, rather than maximum distance from the xylem to the gas exchange surface was used because in conifers, of which stomata are distributed evenly across the needle surfaces, the path length scales with average distance (Brodribb and Jordan 2008).

Table 1: Physical characteristics of needle samples (n = 33 for needle length, width, total area, mass per are and needle density, and n=8 for thickness, cross sectional, mesophyll and endodermis areas) and xylem distance to stomata obtained in the upper crowns of loblolly pine trees, growing under ambient carbon dioxide concentration, elevated and/or N-fertilized conditions (Duke FACE site). Note that the endodermis area corresponds to the areas delimited by the endodermis cells, i.e. the transfusion tissue and the vascular bundle.

	ANOVA						
	Ambient– Unfertilized	Ambient– Fertilized	Elevated– Unfertilized	Elevated– Fertilized	CO ₂	N	CO ₂ xN
Length (cm)	17.4 ± 0.6	19.2 ± 0.8	18.0 ± 0.7	19.7 ± 0.7	0.74	0.02	0.70
Width (mm)	1.52 ± 0.02	1.60 ± 0.03	1.49 ± 0.03	1.61 ± 0.03	0.62	<0.01	0.30
Thickness (mm)	0.81 ± 0.02	0.78 ± 0.03	0.85 ± 0.04	0.82 ± 0.02	0.13	0.37	0.77
Total surface area (mm ²)	4.8 ± 0.1	5.4 ± 0.2	4.7 ± 0.2	5.4 ± 0.2	0.76	0.01	0.56
Mass per area (g m ⁻²)	79.1 ± 2.9	81.0 ± 5.3	81.6 ± 3.5	82.2 ± 6.2	0.78	0.58	0.77
Density (g cm ⁻³)	0.39 ± 0.01	0.41 ± 0.02	0.37 ± 0.01	0.42 ± 0.02	0.85	0.04	0.27
Cross sectional area (mm ²)	0.50 ± 0.01	0.44 ± 0.02	0.48 ± 0.02	0.45 ± 0.02	0.77	0.05	0.57
Mesophyll area (mm ²)	0.34 ± 0.01	0.29 ± 0.01	0.33 ± 0.01	0.30 ± 0.01	0.90	0.02	0.48
Endodermis area (mm ²)	0.15 ± 0.01	0.14 ± 0.01	0.16 ± 0.01	0.15 ± 0.02	0.91	0.34	0.51
Mesophyll fraction (%)	68 ± 2	67 ± 01	69 ± 1	67 ± 1	0.82	0.62	0.58
Xylem Fraction (%)	2.4 ± 0.2	2.6 ± 0.3	1.9 ± 0.1	2.6 ± 0.2	0.39	0.07	0.37
Tracheids per needle	159 ± 9	126 ± 8	117 ± 7	127 ± 19	0.09	0.44	0.18
Xylem to stomata (µm)	296 ± 10	276 ± 5	346 ± 10	321 ± 16	0.06	0.08	0.84

Analysis of variance (ANOVA) probability values for carbon dioxide concentration (CO₂) and N-fertilization treatment (N) are also shown (the probability level $P < 0.15$ was considered to indicate a trend).

Vascular and extravascular leaf conductances

Measurements of leaf hydraulic resistances on a surface area basis (R_{leaf}) was measured using a high pressure flow meter on current-year needles (HPFM; Tsuda and Tyree 2000). We report here R_{leaf} rather than K_{leaf} ($=1/R_{\text{leaf}}$), because resistances add in series, enabling measured values for shoots to be partitioned into their resistance components. Briefly, apical shoots with current year-needles attached were attached to the HPFM (Dynamax Gen2, IN, USA) using a compression fitting. Deionized, degassed, water filtered at 0.1 µm was forced at a pressure of 0.2-0.3 MPa into the shoots through the leaf, and eventually out of the stomata. R_{shoot} (MPa s m² mmol⁻¹) was recorded every 30 s and was shown to increase during the first 3-5 min. Data points were recorded after stable values were reached corresponding to a coefficient of variation <5% for the last 10 readings. Following determination of R_{shoot} , the needles were removed with clean razor blades at its connection to the woody stem, and the hydraulic resistance re-measured (R_{stem}). Measurements typically took 10-15 min for an intact shoot, and additional 5-10 min after needle removal. R_{leaf} was calculated by subtracting R_{stem} from R_{shoot} . R_{stem} never represented more than 7% of R_{shoot} , indicating that most of the hydraulic resistances were located in the leaves. R_{shoot} and R_{leaf} were measured on both control (intact) leaves and on frozen-thawed needles (frozen at -55°C for 10 min and then thawed for 30 min at +23 °C). Freezing the needles removes most of the membrane component of the non-vascular pathways (Tyree et al. 2001, Nardini et al. 2003, Cochard et al. 2004a), and therefore K_{leaf} of frozen needles represents a good estimate of the hydraulic conductance of the vascular water pathway (K_{vascular}). Preliminary tests on four shoots showed that R_{shoot} , once stable, remained so for >20 min, the period during which removing needles and re-measuring were completed. Note that R_{shoot} determined using dionized water was statistically similar (paired t-test: $P=0.19$, $n=7$) to that found using tap water and that illuminating the shoots did not affect R_{shoot} and thus R_{leaf} (paired t-test: $P=0.45$, $n=5$). Using the ohm (electrical resistance) analogy applied to a hydraulic circuit, extravascular conductance ($K_{\text{extravascular}}$) was then calculated as:

$$K_{\text{extravascular}} = (1/K_{\text{leaf}} - 1/K_{\text{vascular}})^{-1} \quad \text{Equation 1}$$

Vascular lumen and bordered-pit conductivity

Hydraulic conductance of coniferous tracheids is a function of both the tracheid lumen conductance and bordered-pit conductance. Total conductivity of a needle lumen is also determined by the aggregate conductivity through a population of conduits, some transporting water and others not. To account for the disproportionate contribution of large conduits to total flow, the first step was to estimate tracheid diameter distributions for calculation of mean hydraulic diameter ($=\Sigma d^5/\Sigma d^4$, where d = individual conduit diameter, Kolb and Sperry 1999). The theoretical lumen xylem conductivity of needle vein on a leaf area basis (K_{lumen}) was calculated according to the Hagen-Poiseuille law using conduit diameter, mean conduit density and the ratio of leaf xylem to leaf area (Lewis and Boose 1995,

Woodruff et al. 2008). Total conductivity of needle is determined by the aggregate conductivity along the entire length. The assumption of equal-sized tracheids holds for much of the needle, but diverged to some degree at the very tip. This divergence induces a correction factor of 0.96 (Zwieniecki et al. 2006) that allows estimation of the integrated K_{lumen} based on the size and number of tracheids measured in the middle section of the needle. Modelling predictions have also shown that pit resistance to water flow in tracheids is not necessarily negligible for conduit diameters ranging from 8-12 μm and, therefore, even in pine needles a significant proportion of the resistance to water flow may be confined in the end-wall (Hacke et al. 2005). We estimated the specific conductivity of the pits, which represents the parallel conductivity of pits (K_{pit}) on a leaf area basis (rather than for individual pits). Measured vascular conductivity was assumed to represent the joint conductivity of both lumen and pits (K_{lumen} and K_{pit} , respectively) and thus K_{pit} could be calculated as:

$$K_{\text{pit}} = (1/K_{\text{vascular}} - 1/K_{\text{lumen}})^{-1} \quad \text{Equation 2}$$

Xylem-wall collapse of vascular bundle conduits

Embolized conduits experience large bending stresses that could lead to cell collapse when water potential drops. Wall collapse reduces lumen area and accordingly considerably increases the hydraulic resistance of tracheid to water flow and K_{vascular} . The conduit thickness-to-span ratio is typically analyzed as a measure of this vulnerability to xylem-wall collapse (Kennedy and Venard 1962). The basis for this relationship is that, the double xylem cell wall shared by adjacent cells behaves in a manner similar to a long plate of width b (tracheid diameter) and thickness t (double cell-wall thickness), and this plate will buckle under a force proportional to $(t/b)^2$ (Hacke et al. 2001). For needle conduits that are circular in shape, it has been proposed that xylem wall collapse is actually proportional to $(t/b)^3$ (Timoshenko and Gere 1961, Brodribb and Holbrook 2005). The shape of the larger cells constituting the vascular bundles were rather square in shape, whereas the smaller tracheids were indeed more cylindrical. Therefore, because we were also interested in tracheids with diameters within 10% of the mean hydraulic diameter, we calculated collapsing pressures for those large tracheids as a function of $(t/b)^2$, and for the others as a function of $(t/b)^3$. The use of tracheids of mean hydraulic diameter as a measure vulnerability to xylem wall collapse is useful because it is this segment of the tracheid population that represent 50% of conductivity (Kolb and Sperry 1999), and thus by collapsing would induce a 50% reduction in K_{vascular} .

Statistical analysis

The effects of CO_2^e and N-fertilization on structural and anatomical features were tested based on an analysis of variance (ANOVA) based on a split-plot design where individual plots were used as replicates. CO_2 concentration and N were the main and split-plot effects, respectively. Probability levels $P < 0.05$, $P < 0.10$ and $P < 0.15$ were considered to indicate a significant effect, a strong tendency, or a trend, respectively. Statistical analyses were performed using SAS (version 9.1, Cary, NC), and curve fits were performed using SigmaPlot (version 12.5, Systat Software, Inc. San Rafael, CA).

Results and Discussion

Our results showed that resource availability affected K_{leaf} by causing differences in leaf xylem anatomy (Pritchard et al. 1998). As previously reported (Maier et al. 2008), CO_2^e had no effect on needle length and width and only a marginal effect on thickness (Table 1). As expected (Chandler and Dale 1996), N-Fertilization increased needle length by 9% and fascicle width by 6%, which translated into a significant increase in total needle surface area (Table 1). Leaves were denser and longer in N-fertilized trees (Table 1). Greater leaf hydraulic conductance (K_{leaf}) under CO_2^a was not associated with greater xylem cross-sectional area, nor lower mass per area. Transverse section of pine needles revealed that the single central vein had two strands of phloem and xylem embedded in transfusion tissue that represented around 15% of the whole surface area across treatments (Table 1, Supplementary Figure 1). In our transverse sections, the chlorophyll-containing mesophyll comprised 68% of the total surface and was not influenced by any of the treatments (Lin et al. 2001). Mesophyll area and needle area were highly correlated, and a common relationship was observed with a slope of 0.70 ± 0.09 across treatments (Figure 1). Overall, needle tracheid sizes ranged from a minimum diameter of $7\mu\text{m}$ to a maximum of $12\mu\text{m}$, with N-fertilization decreasing the mean tracheid diameter by 8% (Table 2), and CO_2^e having a negative discernable effect on the number of tracheids per needle (Table 2; Figure 2A). Tracheid wall thickness and tracheid diameter were positively correlated across treatments ($r^2 = 0.61$, $P < 0.001$) and there was a discernable CO_2^e and a $\text{CO}_2^e \times \text{N}$ interaction effect on cell wall thickness (Table 2, Figure 2B). The distance from the xylem bundle to the stomata increased with CO_2^e , and decreased with N fertilization; however, no interaction was observed (Table 1, Figure 2C). As previously reported (Ceulemans et al. 1994), the mean hydraulic diameter of leaf tracheids and the corresponding tracheid lumen conductivity did not vary among treatments (Table 2).

Table 2: Anatomical characteristics of needle xylem (n=9) obtained in the upper crowns of loblolly pine trees, growing under ambient carbon dioxide concentration, elevated and/or N-fertilized conditions (Duke FACE site). Theoretical tracheid lumen hydraulic conductance based on the Hagen-Poiseuille’s equation (K_{lumen}) and xylem tensions potentially inducing xylem (tracheids) wall collapse are also given.

	Ambient– Unfertilized	Ambient– Fertilized	Elevated– Unfertilized	Elevated– Fertilized	ANOVA		
					CO ₂	N	CO ₂ xN
Cell wall thickness (μm)	1.25 ± 0.02	1.15 ± 0.05	1.33 ± 0.05	1.39 ± 0.08	0.04	0.78	0.06
Hydraulic diameter (μm)	8.5 ± 0.2	7.7 ± 0.1	8.5 ± 0.2	8.0 ± 0.3	0.38	0.02	0.37
K_{lumen} (mmol m ² s ⁻¹ MPa ⁻¹)	15.8 ± 2.9	15.3 ± 2.8	19.9 ± 2.0	16.2 ± 2.8	0.43	0.31	0.41
Xylem collapse pressure (MPa)	-2.14 ± 0.11	-2.27 ± 0.18	-2.43 ± 0.15	-3.00 ± 0.30	0.07	0.07	0.22
Xylem collapse pressure inducing 50% loss of K_{vascular} (MPa)	-1.37 ± 0.07	-1.49 ± 0.11	-1.61 ± 0.08	-1.89 ± 0.11	0.03	0.04	0.29
K_{leaf} (mmol m ² s ⁻¹ MPa ⁻¹)	5.8 ± 0.5	5.3 ± 0.3	4.9 ± 0.3	4.0 ± 0.4	0.07	0.04	0.42
K_{vascular} (mmol m ² s ⁻¹ MPa ⁻¹)	12.4 ± 1.3	10.8 ± 0.2	14.6 ± 2.1	9.8 ± 0.4	0.71	0.03	0.19
$K_{\text{extravascular}}$ (mmol m ² s ⁻¹ MPa ⁻¹)	10.8 ± 1.0	10.7 ± 1.5	8.3 ± 1.0	6.9 ± 0.9	0.04	0.53	0.56
% $K_{\text{extravascular}}$	54 ± 2	51 ± 4	62 ± 6	59 ± 2	0.03	0.56	0.99

Analysis of variance (ANOVA) probability values for carbon dioxide concentration (CO₂) and N-fertilization treatment (N) are also shown.

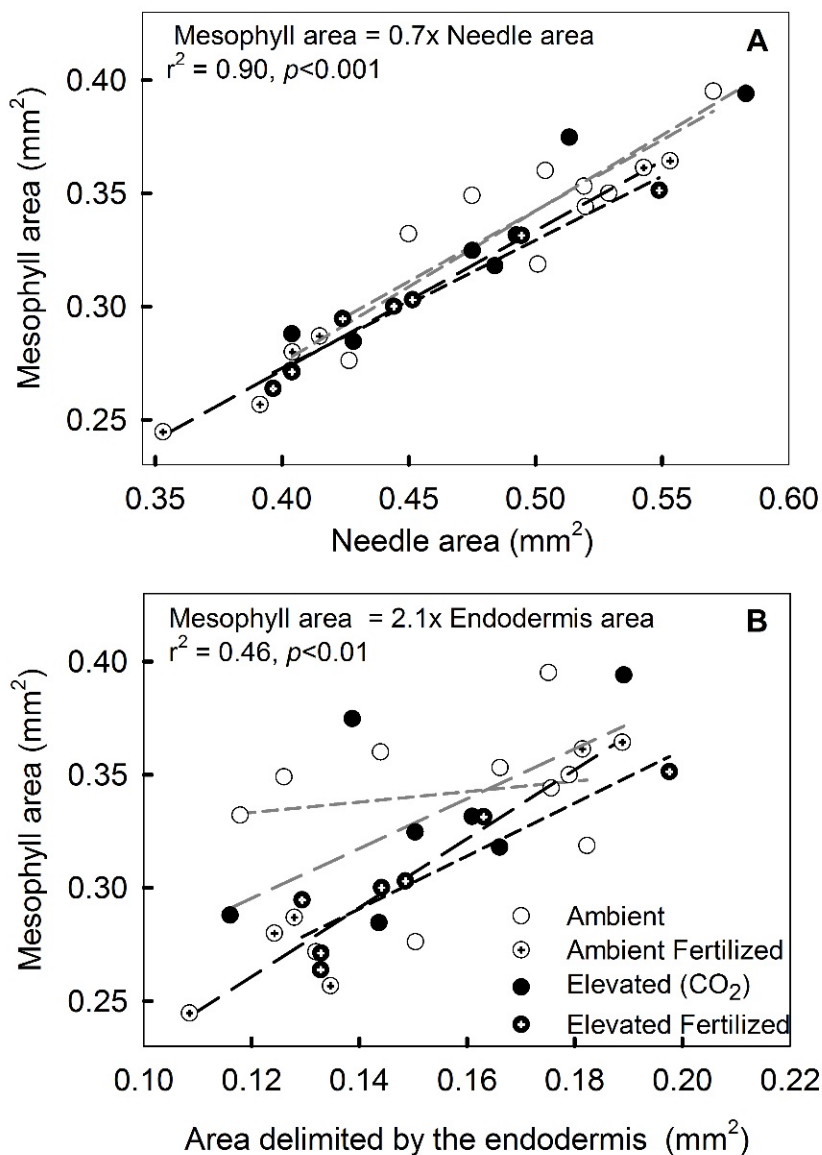


Figure 1: Relationship between (A) mesophyll area and needle area, and between (B) mesophyll area and endodermis area of *Pinus taeda* (loblolly pine) needles grown under elevated CO₂ and under N-fertilization. Note: area delimited by the endodermis corresponds to the area surrounded by the endodermis cells, i.e. the transfusion tissue and the vascular bundle (See Supplementary Figure 1). A regression line is drawn for each treatment. The slopes of the relationships between mesophyll area and needle area ranged from 0.79 in ambient CO₂, to 0.69 in ambient CO₂-fertilized, 0.89 in elevated CO₂ and 0.65 in elevated CO₂-fertilized. All intercepts were not significantly different from zero. In (A), no differences were found in the slopes of the regression lines. In (B), ambient leaves had a shallower slope ($P=0.036$) than the other three treatments (Tukey–Kramer test).

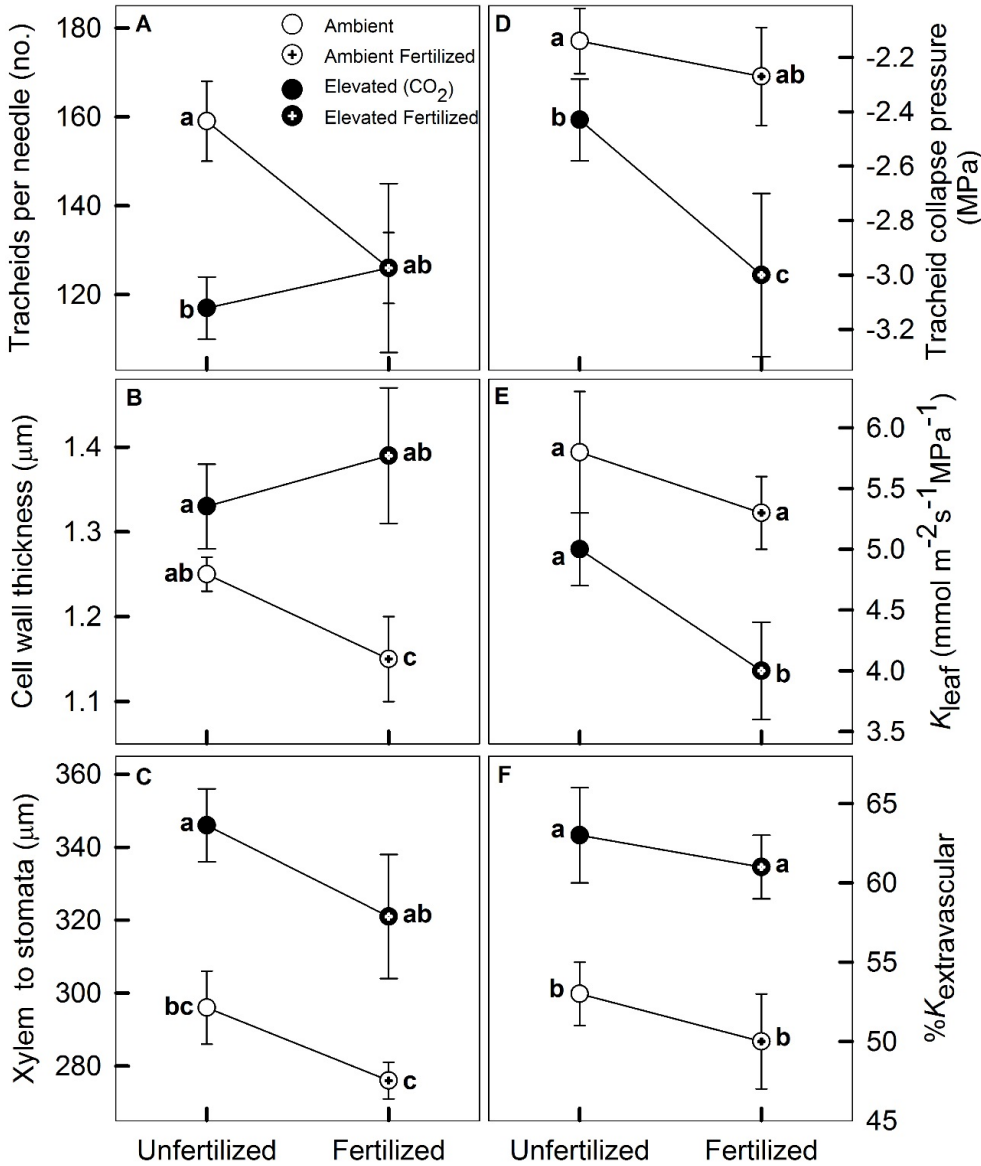


Figure 2: Treatment mean of physical and anatomical parameters of *Pinus taeda* (loblolly pine) needles described in Tables 1 and 2. Variables are expressed in relation to N-fertilization treatment on the x-axis. Means accompanied by different letters indicate a significant effect (least square means significant difference, $P < 0.05$). Error bars represent standard error of the mean. Trends for K_{vascular} and for the Tracheid Collapse Pressure inducing 50% loss of K_{vascular} followed the same trends as $\%K_{\text{extravascular}}$ (panel F) and Tracheid Collapse Pressure (Panel D), respectively.

Consistent with earlier observations at the site (Domec et al. 2009a), CO₂^e and N had a strong negative effect on maximum K_{leaf} (Table 2, Figure 2E); however, no interaction was discernable. The freezing method was effective for determining $K_{\text{extravascular}}$, but, contrary to our first hypothesis, treatment varied in the proportion of K_{vascular} to K_{leaf} ; 51% (CO₂^a) to 64% (CO₂^e) of the hydraulic resistances were located outside the vascular bundle (Table 2, Figure 3A). The decline in K_{leaf} under CO₂^e was driven by the decline in $K_{\text{extravascular}}$ rather than a decline in K_{vascular} (Figure 4). It is interesting to note that the reduction in K_{leaf} under CO₂^e was roughly on the same order of magnitude as the increase in the contribution of $K_{\text{extravascular}}$, meaning that in absolute terms K_{vascular} did not vary with CO₂^e (Table 2, Figure 4).

Following our second hypothesis, the decline of $K_{\text{extravascular}}$ under CO₂^e explained the decline of stomatal conductance (g_s) under CO₂^e (Figure 3B). The underlying causes of smaller g_s under CO₂^e has been elusive (Domec et al. 2010, Ward et al. 2013), until recently when Tor-ngern et al. (2015) demonstrated an indirect effect of CO₂^e on g_s . Regardless of soil moisture or leaf water status, CO₂^e was shown to induce a 25% reduction in K_{leaf} of *Pinus taeda*, which was large enough to explain the observed long term reduction in g_s . Treatment-induced adjustments increased the path length of water movement from the xylem bundle to the stomata (Table 2), therefore potentially explaining the increase in resistance along radial extravascular hydraulic pathway (Brodrribb et al. 2007, Buckley et al. 2011). This physical constrain to water movement from the xylem to the stomata under CO₂^e may be the mechanistic explanation for the indirect effect of CO₂^e on g_s (Tor-ngern et al. 2015), a previously unrecognized acclimation to changing climate.

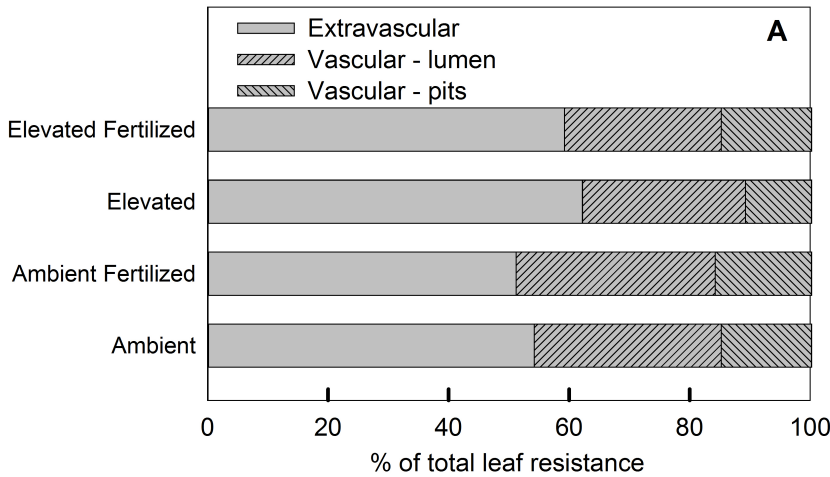


Figure 3: (A) Proportion of vascular (xylem) and extravascular (outside xylem) hydraulic resistances to the overall leaf hydraulic resistance ($1/K_{leaf}$) and (B) reference stomatal conductance (g_s at a vapor pressure deficit of 1 kPa, taken from Domec et al. 2009a) versus the extravascular hydraulic conductance in *Pinus taeda* (loblolly pine) needles grown under elevated CO_2 and under N-fertilization.

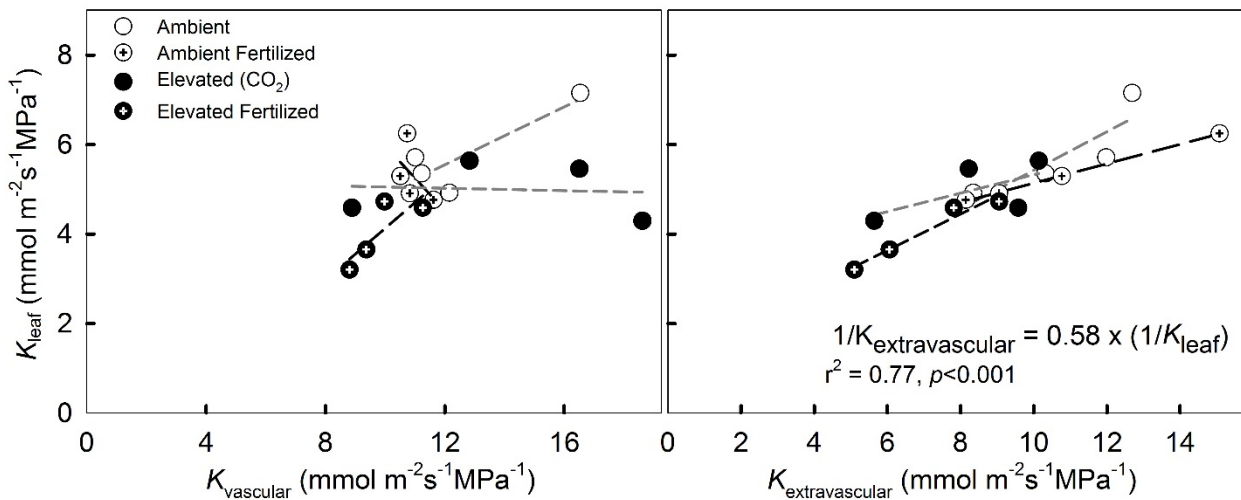
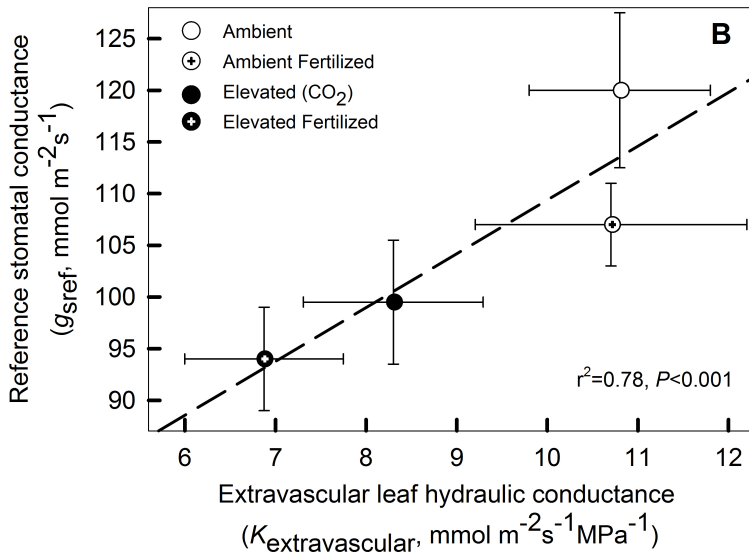


Figure 4: Relationship between leaf hydraulic conductance (K_{leaf}) and vascular ($K_{vascular}$) and extravascular ($K_{extravascular}$) hydraulic conductances of *Pinus taeda* (loblolly pine) needles grown under elevated CO_2 and under N-fertilization. A regression line is drawn for each treatment. For the relationships between K_{leaf} and $K_{extravascular}$ no difference was found in slopes of regression lines between treatments (Tukey–Kramer test).

A hydraulic model suggested that, species with a leaf hydraulic design limited by $K_{\text{extravascular}}$ should be better suited to supply water evenly throughout the leaf (Cochard et al. 2004a, Buckley et al. 2011), increasing stomata sensitivity to environmental changes (Mott and Buckley 2000). Furthermore, previous studies have suggested that evaporation of water into substomatal cavities occurs mainly in the vicinity of the guard cells (Meidner and Edwards 1975, Tyree & Yianoulis 1980, Dewar 2002). This peristomatal transpiration implies that the water potential difference between the leaf epidermis and the guard cells is proportional to the membrane hydraulic conductivity (Heidecker et al. 2003). It is therefore expected that $K_{\text{extravascular}}$ should decline as water potential falls, describing the effects of leaf dehydration and declining cell turgor on membrane permeability (Pantin et al. 2012, Rockwell et al. 2014). Our previous results showed that K_{leaf} declines faster as leaf water potential drops under CO_2° and N-fertilization (Domec et al. 2009a), which could also be explained by the proportionally greater extravascular resistance to leaf water flow (Table 2, Figure 2F). Faster decline of K_{leaf} under CO_2° and N-fertilization may be the consequence of the bundle sheath and mesophyll cells losing turgor and shrinking, thus mechanically increasing resistance to water flow (Brodribb and Holbrook 2004, Scoffoni et al. 2011). The concept of a turgor-limited passage through the bundle sheath and mesophyll is supported by the correlations between the point of turgor loss and K_{leaf} (Brodribb and Holbrook 2003, Woodruff et al. 2007, Domec et al. 2009a, Scoffoni et al. 2011).

Hydraulic conductance of the vascular tissues depends on both the lumen conductance and the pit membrane conductance. In some species, pit membrane conductivity of xylem in roots and branches is more limiting in trees growing under CO_2° conditions (Domec et al. 2010). Across treatment our results showed that needle vein conductivity was slightly more limited by the conduit lumen than by bordered-pit resistance, because pit resistance accounted for only 30-45% of vein resistance. Overall, pit resistance accounted for less than 17% of K_{leaf} (Figure 3A). There was no CO_2° nor N-fertilization effect on needle pit resistance ($P>45$). We are unaware of another study that have quantified the contribution of end-wall resistance to the overall leaf resistance to water flow in leaves. The low pit resistance suggested that inter-tracheid bordered-pit membranes in loblolly pine leaves may be composed of a thin torus, a small ratio of torus to pit aperture diameter and a weak cell wall (Hacke et al. 2005, Pittermann et al. 2006, Domec et al. 2008, Bouche et al. 2014). These microscopic cell-wall anatomical features would likely minimize pit resistance to water flow, thus enhancing K_{vascular} , but they would also increase the risk of air-seeding and xylem wall collapse. Inter-conduit pits allow water flow between vessels, but in conifers they also act as safety valves to prevent the spreading of air from embolized vessels (Domec et al. 2006, Delzon et al. 2010).

Our study revealed that CO_2° caused thicker tracheid cell walls and thus a change in collapse pressures (Table 2). Xylem collapse pressures decreased with CO_2° , and also with N fertilization, but no interaction effect was observed (Table 2; Figure 2D). Following our third hypothesis, treatment-induced reductions in K_{leaf} were consistent with increased resistance to xylem-wall collapse (Figure 5A) and, therefore, stomatal closure corresponded to a 50% collapse of needle tracheids (Figure 5B). The calculated collapsing pressures required to reduce significantly K_{vascular} were also strongly correlated with the measured tensions at which g_s in the field began to decline (Figure 5B), suggesting that the collapse of needle tracheids could explain the midday depression in K_{leaf} and g_s . If we assume that leaf resistance comprises up to 40% of the whole-tree resistance (Sack and Holbrook 2006, Domec et al. 2009a), then the pressure inducing 50% loss of K_{vascular} would lower tree conductance by less than 20%. Therefore, this decline in K_{vascular} is steep enough to create a hydraulic signal triggering stomata closure without compromising the whole-tree hydraulic integrity and thus without preventing g_s from reaching its maximum. The physiological significance of xylem-wall collapse under field condition may be its role as part of the hydraulic signals that trigger stomatal closure (Cochard et al. 2004b). Treatment-induced anatomical adjustments, such as a the decrease in tracheid fraction and an increase in cell-wall thickness under CO_2° , are consistent with a significant trade-off in conifer wood structure between attaining greater mechanical reinforcement (i.e. higher thickness:span, or wood density) at the expense of reduced hydraulic efficiency (Pittermann et al. 2006, Domec et al. 2009b, Rosner et al. 2016). It should be noted, however, that our calculated xylem-wall collapse pressures may be overestimated due to the use of imprecise value of single-fiber mechanical properties (Jayne 1959, Mott et al. 2002). In actual tracheids, bordered-pits between adjacent cells create cell wall imperfections, causing an interaction between plasticity and instability, making the failure pressure smaller than the theoretical values (Yeh and Kyriakides 1988, Corradi et al. 2005). Furthermore, anatomical adjustments following CO_2° induced an 11-25% increase in cell wall thickness (Table 2) and, thus, in the water potentials that would induce total xylem-wall collapse (Figure 2E). Because thick and stiff cell walls have been shown to reduce turgor loss (Marshall and Dumbroff 1999), this could also explain the lower water potential at turgor loss (Figure 5C). Again, these correlations support the concept of a turgor-limited passage through the bundle sheath and mesophyll (Brodribb and Holbrook 2005, Woodruff et al. 2007, Leigh et al. 2011).

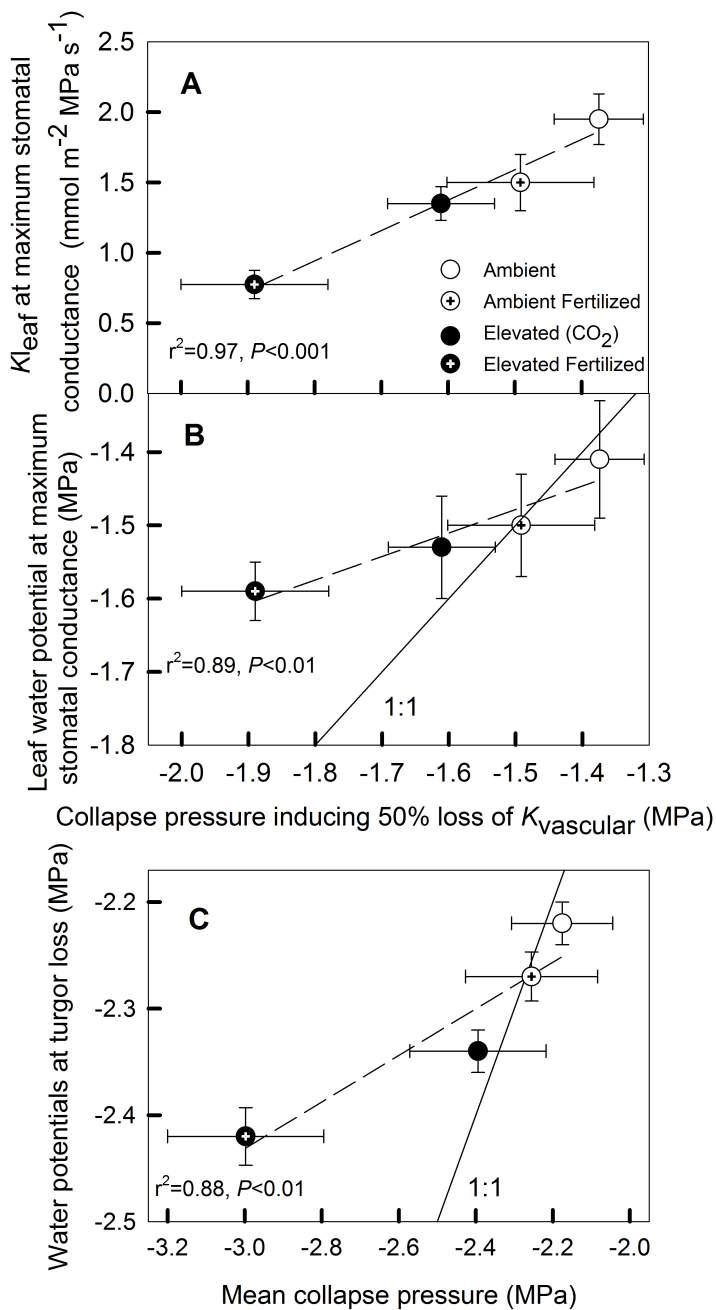


Figure 5: Relationships among hydraulic properties of *Pinus taeda* (loblolly pine) needles. (A) Leaf hydraulic conductance (K_{leaf}) and (B) leaf water potential at stomatal closure versus the pressure required to collapse tracheids representing 50% of K_{vascular} (collapse pressure inducing a 50% reduction in K_{vascular}). (C) Shows the relationship between leaf water potential at turgor loss versus the pressure required to collapse all xylem (mean collapse pressure). Data for K_{leaf} and leaf water potential at maximum g_s as well as data for water potentials at turgor loss are from Domec et al. (2009a).

The strong correlations between K_{leaf} and xylem-wall collapse (Figure 5A) add weight to other studies suggesting that conduit collapse can contribute to decreasing K_{leaf} as leaf water potential declines (Brodrribb and Holbrook 2005, Scoffoni et al. 2014). From Figure 5A, it can be seen that xylem-wall collapse could reduce K_{leaf} by 45%, via the total decline in K_{vascular} , which could then mirror the reduction in $K_{\text{extravascular}}$ (described above) as leaf water potentials drops. Although the mechanism explaining the reduction in K_{vascular} with leaf water potential likely involves cavitation-induced embolism (Woodruff et al. 2007, Johnson et al. 2009), we cannot rule out that leaf xylem might also collapsed at lower water potential. It has been suggested that the collapse of needle tracheids could be an adaptive means of regulating leaf water potential without risking embolism. Being a mechanical process, cell-deformation could be restored elastically as water potentials are relaxed, whereas the refilling embolized conduits is unlikely. Although recent image analyses showed that tracheid deformation could potentially only occur in seedlings (Bouche et al. 2015), a few other studies have experimentally demonstrated that the theoretical collapse pressure for pine needle tracheids and the surrounding transfusion tissue, calculated from equations that describe cell wall resistance to bending and pipe buckling under tension (Timoshenko and Gere 1961, Hacke et al. 2001), corresponded to actual cell collapse observed during leaf dehydration (Cochard et al. 2004b, Brodrribb and Holbrook 2005). What is still unclear, however, is why tracheid cell wall in needles is small relative to lumen diameter as compared to other plant organs where it can be up to three times as large (Hacke et al. 2005, Domec et al. 2010). Usually, the smaller the tracheid lumen, the higher the mean collapse pressure. Recently, Zhang et al. (2014) demonstrated that the collapse of

transfusion tissue (that is present in all gymnosperms) can also significantly affect K_{leaf} . Because these cells are in direct contact with the xylem bundle, one can hypothesize a direct link between the collapse of the two adjacent tissues, thus creating a concomitant change in K_{vascular} and $K_{\text{extravascular}}$.

Conclusions

Utilizing unique experimental settings, such as FACE, to examine the effect of CO_2° on plant structure increases our ability to forecast future environmental impacts on forest growth and function. We showed that long-term acclimation to CO_2° altered the structure and anatomy of loblolly pine leaves, impacting the leaf hydraulic system and affecting stomatal conductance. We show evidence that CO_2° and N-Fertilization treatments induced a decrease in leaf hydraulic capacity and also decreased the conductance to water flow from the xylem to the leaf-internal air space. This contrasts with previous studies focusing on a direct stomatal response to CO_2° . These findings suggest that structural adjustments to CO_2° and their consequences to gas exchange must be incorporated in models employed to predict forest responses to climate change.

Acknowledgements

This research was supported by the Office of Science (BER and TES) of the US Department of Energy through the Southeastern Regional Center (SERC) of the National Institute for Global Environmental Change (NIGEC), and through Terrestrial Carbon Processes (TCP) program. This research was also supported by NSF-EAR-1344703 and NSF-IOS-1549971 and grants from the French Research Agency (MACACC ANR-13-AGRO-0005 and MARIS ANR-14-CE03-0007).

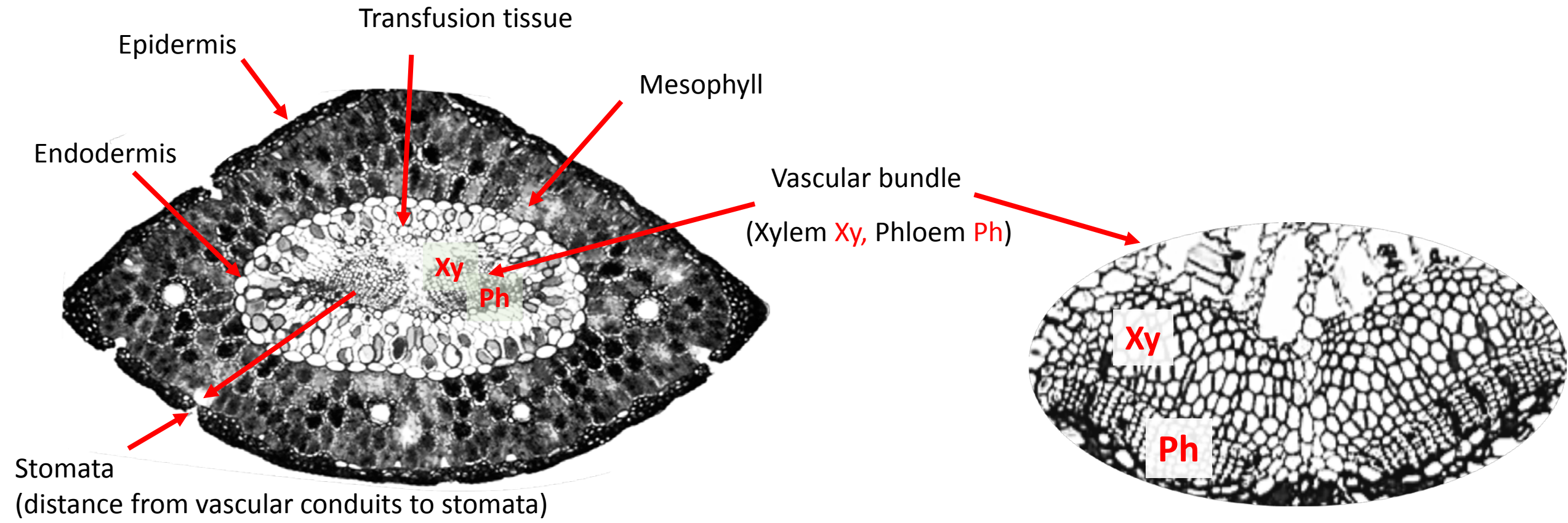
References

- Addington RN, Mitchell RJ, Oren R, Donovan LA. 2004. Stomatal sensitivity to vapor pressure deficit and its relationship to hydraulic conductance in *Pinus palustris*. *Tree Physiology* 24: 561–569
- Aasamaa K, Sober A, Rahi M. 2001. Leaf anatomical characteristics associated with shoot hydraulic conductance, stomatal conductance and stomatal sensitivity to changes of leaf water status in temperate deciduous trees. *Australian Journal of Plant Physiology* 28: 765–774
- Bouche PS, Larter M, Domec JC, Burlett R, Gasson P, Delzon S. 2014. Increased hydraulic safety implies high xylem mechanical resistance but limited impact on hydraulic efficiency in conifers. *Journal of Experimental Botany* 65: 4419–4431
- Bouche PS, Delzon S, Choat B, Badel E, Brodribb T, Burlett R, Cochard H, Charra-Vaskou K, Lavigne B, Li S, Mayr S, Morris H, Torres-Ruiz J, Zufferey V, Jansen S. 2016. Are needles of *Pinus pinaster* more vulnerable to xylem embolism than branches? New insights from X-ray computed tomography. *Plant, Cell & Environment* doi: 10.1111/pce.12680
- Brodribb TJ, Jordan GJ. 2008. Internal coordination between hydraulics and stomatal control in leaves. *Plant, Cell & Environment* 31:1557–1564
- Brodribb TJ, Holbrook NM. 2003. Stomatal closure during leaf dehydration, correlation with other leaf physiological traits. *Plant Physiology* 132: 2166–2173
- Brodribb TJ, Holbrook NM. 2004. Diurnal depression of leaf hydraulic conductance in a tropical tree species. *Plant, Cell & Environment* 27: 820–827
- Brodribb TJ, Holbrook NM. 2005. Water stress deforms tracheids peripheral to the leaf vein of a tropical conifer. *Plant Physiology* 137: 1139–1146
- Brodribb TJ, Field TS, Jordan GJ. 2007. Leaf maximum photosynthetic rate and venation are linked by hydraulics. *Plant Physiology* 144: 1890–1898
- Bucci SJ, Scholtz FG, Goldstein G, Meinzer FC, Sternberg L. 2003. Dynamic changes in hydraulic conductivity in petioles of two savanna tree species: factors and mechanisms contributing to the refilling of embolized vessels. *Plant, Cell & Environment* 26: 1633–1645
- Buckley TN, Sack L, Gilbert ME. 2011. The role of bundle sheath extensions and life form in stomatal responses to leaf water status. *Plant Physiology* 156: 962–973
- Buckley TN. 2015. The contributions of apoplastic, symplastic and gas phase pathways for water transport outside the bundle sheath in leaves. *Plant, Cell & Environment* 38: 7–22

- Ceulemans R, Mousseau M. 1994. Effects of elevated atmospheric CO₂ on woody plants. *New Phytologist* 127: 425–446
- Chandler JW, Dale JE. 1996. Nitrogen deficiency and fertilization effects on needle growth and photosynthesis in Sitka spruce (*Picea sitchensis*). *Tree Physiology* 15: 813–817
- Charra-Vaskou K, Badel E, Burrell R, Cochard H, Delzon S, Mayr S. 2012. Hydraulic efficiency and safety of vascular and non-vascular components in *Pinus pinaster* leaves. *Tree Physiology* 32: 1161–1170
- Cochard H, Nardini A, Coll L. 2004a. Hydraulic architecture of leaf blades: where is the main resistance? *Plant, Cell & Environment* 27: 1257–1267
- Cochard H, Froux F, Mayr S, Coutand C. 2004b. Xylem wall collapse in water-stressed Pine Needles. *Plant Physiology* 134: 401–406
- Corradi L, Luzzi L, Rudi F. 2005. Collapse of thick cylinders under radial pressure and axial load”, *ASME. Journal of Applied Mechanics* 72: 564–569
- Coomes DA, Heathcote S, Godfrey ER, Shepherd JJ, Sack L. 2008. Scaling of xylem vessels and veins within the leaves of oak species. *Biological Letters* 4: 302–306
- Delzon S, Douthe C, Sala A, Cochard H. 2010. Mechanism of water-stress-induced cavitation in conifers: bordered pit structure and function support the hypothesis of seal-capillary seeding. *Plant, Cell & Environment* 33: 2101–2111
- Dewar RC. 2002. The Ball–Berry–Leuning and Tardieu–Davies stomatal models: synthesis and extension within a spatially aggregated picture of guard cell function. *Plant, Cell & Environment* 25: 1383–1398
- Domec J-C, Lachenbruch B, Meinzer FC. 2006. Bordered pit structure and function determine spatial patterns of air-seeding thresholds in xylem of Douglas-fir (*Pseudotsuga menziesii*; Pinaceae) trees. *American Journal of Botany* 93: 1588–1600
- Domec J-C, Prunyn ML. 2008. Bole girdling affects metabolic properties and root, trunk and branch hydraulics of young ponderosa pine trees. *Tree Physiology* 28: 1493–1504
- Domec J-C, Lachenbruch B, Meinzer FC, Warren JM, Woodruff DR, McCulloh KA. 2008. Maximum height in a conifer is associated with conflicting requirements for xylem design. *Proceedings of the National Academy of Sciences USA* 105: 12069–12074
- Domec J-C, Palmroth S, Ward E, Maier CA, Thereuzien M, Oren R. 2009a. Interactive effects of long term elevated CO₂ and N-fertilization on the coordination between leaf hydraulic conductance and stomatal conductance in *Pinus taeda*. *Plant, Cell and Environment* 32: 1500–1512
- Domec J-C, Warren J, Lachenbruch B, Meinzer FC. 2009b. Safety factors from air seeding and cell wall implosion in young and old conifer trees. *IAWA Journal* 30: 100–120
- Domec J-C, Schafer K, Oren R, Kim H, McCarthy H. 2010. Variable conductivity and embolism in roots and branches of four contrasting tree species and their impacts on whole-plant hydraulic performance under future atmospheric CO₂ concentration. *Tree Physiology* 30: 1001–1015
- Hacke UG, Sperry JS, Pockman WT, Davis SD, McCulloh KA. 2001. Trends in wood density and structure are linked to prevention of xylem implosion by negative pressure. *Oecologia* 126: 457–461
- Hacke UG, Sperry JS, Pittermann J. 2005. Efficiency versus safety tradeoffs for water conduction in angiosperm vessels versus gymnosperm Tracheids. In: Holbrook NM, Zwieniecki MA (eds.), *Vascular Transport in Plants*. USA: Elsevier Academic Press. pp. 333–354
- Heidecker M, Wegner LH, Binder KA, Zimmermann U. 2003. Turgor pressure changes trigger characteristic changes in the electrical conductance of the tonoplast and the plasmalemma of the marine alga *Valonia utricularis*. *Plant, Cell & Environment* 26: 1035–1051
- Jacobsen AL, Ewers EW, Pratt RB, Paddock WA, Davis SD. 2005. Do xylem fibers affect vessel cavitation resistance? *Plant Physiology* 139: 546–556
- Jayne BA. 1959. Mechanical properties of wood fibers. *Tappi* 42: 461–467
- Johnson DM, Meinzer FC, Woodruff DR, McCulloh KA. 2009. Leaf xylem embolism, detected acoustically and by cryo-SEM, corresponds to decreases in leaf hydraulic conductance in four evergreen species. *Plant, Cell & Environment* 32: 828–836
- Johnson DM, McCulloh KA, Meinzer FC, Woodruff DR, Eissenstat DM. 2011. Hydraulic patterns and safety margins, from stem to stomata, in three eastern US tree species. *Tree Physiology* 31: 659–668
- Johnson DM, McCulloh KA, Woodruff DR, Meinzer FC. 2012. Evidence for xylem embolism as a primary factor in dehydration-induced declines in leaf hydraulic conductance. *Plant, Cell & Environment* 35: 760–769
- Johnson DM, Woodruff DR, McCulloh KA, Meinzer FC. 2009. Leaf hydraulic conductance, measured in situ, declines and recovers daily: leaf hydraulics, water potential and stomatal conductance in four temperate and three tropical tree species. *Tree Physiology* 29: 879–887

- Kennedy CR, Venard JT. 1962. Collapse of tubes by external pressures. Governmental report from Oak Ridge National Laboratory, Oak Ridge, Tennessee. P35
- Kolb KJ, Sperry JS. 1999. Transport constraints on water use by the Great Basin shrub, *Artemisia tridentata*. *Plant, Cell & Environment* 22: 925–925
- Leigh A, Zwieniecki MA, Rockwell FE, Boyce CK, Nicotra AB, Holbrook NM. 2011. Structural and hydraulic correlates of heterophylly in *Ginkgo biloba*. *New Phytologist* 189: 459–470
- Lewis AM, Boose ER. 1995. Estimating volume flow rates through xylem conduits. *American Journal of Botany* 82: 1112–1116
- Lin J, Jach ME, Ceulemans R. 2001. Stomatal density and needle anatomy of Scots pine (*Pinus sylvestris*) are affected by elevated CO₂. *New Phytologist* 150: 665–674
- Leegood RC. 2008. Roles of the bundle sheath cells in leaves of C₃ plants. *Journal of Experimental Botany* 59: 1663–1673
- Maier CA, Palmroth S, Ward E. 2008. Branch growth and gas exchange in 13-year-old loblolly pine (*Pinus taeda*) trees in response to elevated carbon dioxide concentration and fertilization. *Tree Physiology* 28: 1093–1106
- Marshall JG, Dumbroff E.B. 1999. Turgor Regulation via Cell Wall Adjustment in White Spruce. *Plant Physiology* 119: 313–320
- Meidner H, Edwards M. 1975. Direct measurements of turgor pressure potentials of guard cells. I. *Journal of Experimental Botany* 26: 319–330
- Meinzer FC. 2003. Functional convergence in plant responses to the environment. *Oecologia* 134: 1–11
- McCulloh KA, Johnson DM, Petitmermet J, McNellis B, Meinzer FC, Lachenbruch B. 2015. A comparison of hydraulic architecture in three similarly sized woody species differing in their maximum potential height. *Tree Physiology* 35: 723–731
- Mott KA and Buckley TN. 2000. Patchy stomatal conductance: emergent collective behaviour of stomata. *Trends in Plant Science* 5: 258–262
- Mott L, Groom L, Shaler S. 2002. Mechanical properties of individual southern pine fibers. Part II. Comparison of earlywood and latewood fibers with respect to tree height and juvenility. *Wood and Fiber Science* 34: 221–237
- Nardini A, Salleo S. 2005. Water stress-induced modifications of leaf hydraulic architecture in sunflower: coordination with gas exchange. *Journal of Experimental Botany* 56: 3093–3101
- Nardini A, Salleo S, Raimondo F. 2003. Changes in leaf hydraulic conductance correlate with leaf vein embolism in *Cercis siliquastrum* L. *Trees Structure and Function* 17: 529–34
- Oren R, Ellsworth DS, Johnsen KH, Phillips N, Ewers BE, Maiers C, Schafer KVR, McCarthy H, Hendrey G, McNulty SG, Katul GG. 2001. Soil fertility limits carbon sequestration by forest ecosystems in a CO₂-enriched atmosphere. *Nature* 411: 469–472
- Pantin F, Monnet F, Jannaud D, Costa JM, Renaud J, Muller B, Simonneau T, Genty B. 2013. The dual effect of abscisic acid on stomata. *New Phytologist* 197: 65–72
- Pittermann J, Sperry J, Wheeler J, Hacke U, Sikkema E. 2006. Mechanical reinforcement of tracheids compromises the hydraulic efficiency of conifer xylem. *Plant, Cell & Environment* 29: 1618–1628
- Prado K, Maurel C. 2013. Regulation of leaf hydraulics: from molecular to whole plant levels. *Frontiers in Plant Science* 4: 255
- Pritchard SG, Mosjidis C, Peterson CM, Runion GB, Rogers HH. 1998. Anatomical and morphological alterations in longleaf pine needles resulting from growth in elevated CO₂: Interactions with soil resource availability. *International Journal of Plant Sciences* 159: 1002–1009
- Pritchard SG, Rogers HH, Prior SA, Peterson CM. 1999. Elevated CO₂ and plant structure: a review. *Global Change Biology* 5: 807–837
- Radoglou KM, Jarvis PG. 1990. Effects of CO₂ enrichment on four poplar clones. I. Growth and leaf anatomy. *Annals of Botany* 65: 617–626
- Reid CD, Maherali H, Johnson HB, Smith SD, Wullschlegler SD, Jackson RB. 2003. On the relationship between stomatal characters and atmospheric CO₂. *Geophysical Research Letters* 30: 1–4
- Rockwell FE, Holbrook NM, Stroock AD. 2014. Leaf hydraulics. I. Scaling transport properties from single cells to tissues. *Journal of Theoretical Biology* 340: 251–266
- Rosner S, Luss S, Světlík J, Andreassen K, Børja I, Dalsgaard L, Evans R, Tveito OE, Solberg S. 2016. Chronology of hydraulic vulnerability in trunk wood of conifer trees with and without symptoms of top dieback. *Journal of Plant Hydraulics* 3: e001
- Rundel PW, Stecker RE. 1977. Morphological adaptations of tracheid structure to water stress gradients in the crown of *Sequoiadendron giganteum*. *Oecologia* 27: 135–139

- Rundel PW, Yoder BJ. 1998. Ecophysiology of *Pinus*. In Ecology and Biogeography of *Pinus*. Ed. D.M. Richardson. Cambridge University Press, Cambridge, pp 296–323
- Sack L, Cowan PD, Jaikumar N, Holbrook NM. 2003. The ‘hydrology’ of leaves: co-ordination of structure and function in temperate woody species. *Plant, Cell & Environment* 26: 1343–1356
- Sack L, Tyree MT. 2005. Leaf hydraulics and its implications in plant structure and function. Vascular Transport in Plants (eds NM Holbrook & MA Zwieniecki), pp. 564. Elsevier, New York
- Sack L, Holbrook NM. 2006. Leaf hydraulics. *Annual Review of Plant Biology* 57: 361–381
- Sack L, Scoffoni C, Johnson D, Buckley T, Brodribb T. 2015. The anatomical determinants of leaf hydraulic function. Pages 255–271 in U. Hacke, editor. Functional and Ecological Xylem Anatomy. Springer, New York
- Schäfer KVR, Oren R, Lai C-T, Katul GG. 2002. Hydrologic balance in an intact temperate forest ecosystem under ambient and elevated atmospheric CO₂ concentration. *Global Change Biology* 8: 895–911
- Scoffoni C, Rawls M, McKown A, Cochard H, Sack L. 2011. Decline of leaf hydraulic conductance with dehydration: relationship to leaf size and venation architecture. *Plant Physiology* 156: 832–843
- Scoffoni C, Vuong C, Diep S, Cochard H, Sack L. 2014. Leaf shrinkage with dehydration: coordination with hydraulic vulnerability and drought tolerance. *Plant Physiology* 164: 1772–1788
- Scoffoni C. 2015. Modelling the outside-xylem hydraulic conductance: towards a new understanding of leaf water relations. *Plant, Cell & Environment* 38: 4–6
- Tor-ngern, P, Oren R, Ward E, Palmroth S, McCarthy H, Domec J-C. 2015 Increases in atmospheric CO₂ have little influence on transpiration of a temperate forest canopy. *New Phytologist* 205: 215–218
- Timoshenko S, Gere JM. 1961. *Theory of Elastic Stability*, McGraw-Hill, New York
- Thomas JF, Harvey CH. 1983. Leaf anatomy of four species grown under continuous CO₂ enrichment. *Botanical Gazette* 144: 303–309
- Tsuda M, Tyree MT. 2000. Plant hydraulic conductance measured by the high pressure flow meter in crop plants. *Journal of Experimental Botany* 51: 823–828
- Tyree MT, Yianoulis P. 1980. The site of water evaporation from sub-stomatal cavities, liquid path resistances and hydroactive stomatal closure. *Annals of Botany* 46: 175–193
- Tyree MT, Nardini A, Salleo S. 2001. Hydraulic architecture of whole plants and single leaves. In *l’Arbre 2000 the Tree*, ed. Labrecque M, pp. 215–221. Montreal: Isabelle Quentin Publisher
- Woodward FI, Kelly CK. 1995. The responses of stomatal density to CO₂ partial pressure. *New Phytologist* 131: 311–327
- Woodruff DR, McCulloh KA, Warren JM, Meinzer FC, Lachenbruch B. 2007. Impacts of tree height on leaf hydraulic architecture and stomatal control in Douglas-fir. *Plant, Cell & Environment* 30: 559–569
- Woodruff DR, Meinzer FC, Lachenbruch B. 2008. Height-related trends in leaf xylem anatomy and shoot hydraulic characteristics in a tall conifer: safety versus efficiency in water transport. *New Phytologist* 180: 90–99
- Yeh MK, Kyriakides S. 1988. Collapse of deep water pipelines. *ASME, Journal of Energy Resources Technology* 110: 158–164
- Zhang Y-J, Rockwell FE, Wheeler JK, Holbrook NM. 2014. Reversible deformation of transfusion tracheids in *Taxus baccata* is associated with a reversible decrease in leaf hydraulic conductance. *Plant Physiology* 165: 1557–1565
- Zimmermann H. 1983. Xylem structure and the ascent of sap. Berlin: Springer-Verlag. 143p
- Zwieniecki MA, Melcher PJ, Boyce CK, Sack L, Holbrook NM. 2002. The hydraulic architecture of the leaf venation in *Laurus nobilis* L. *Plant, Cell & Environment* 25: 1445–1450
- Zwieniecki MA, Stone HA, Leigh A, Boyce CK, Holbrook NM. 2006. Hydraulic design of pine needles: one-dimensional optimization for single-vein leaves *Plant, Cell & Environment* 29: 803–809
- Zwieniecki MA, Brodribb TJ, Holbrook NM. 2007. Hydraulic design of leaves: insights from rehydration kinetics. *Plant, Cell & Environment* 30: 910–921



Supplementary Figure 1: transverse section of a loblolly pine (*Pinus taeda*) needle indicating the anatomical traits measured (total surface area, mesophyll area, endodermis area, transfusion tissue, vascular bundle, distance from vascular conduits to stomata sub-cavity, number of xylem tracheids).